Published in final edited form as:

Brain Struct Funct. 2017 March ; 222(2): 781–798. doi:10.1007/s00429-016-1246-5.

Maternally involved galanin neurons in the preoptic area of the rat

Melinda Cservenák[#1,2], **Viktor Kis**[#1,3], **Dávid Keller**[1,2], **Diána Dimén**[1,3], **Lilla Menyhárt**[3], **Szilvia Oláh**[1], **Éva R. Szabó**[1,2], **János Barna**[2], **Éva Renner**[4,5], **Ted B. Usdin**[6], and **Arpád Dobolyi**[1,2]

[1] MTA-ELTE NAP B Laboratory of Molecular and Systems Neurobiology, Department of Physiology and Neurobiology, Hungarian Academy of Sciences and Eötvös Loránd University, Budapest, Hungary

[2] Laboratory of Neuromorphology, Department of Anatomy, Histology and Embryology, Semmelweis University, 1094 Budapest, Hungary

[3] Department of Anatomy, Cell and Developmental Biology, Institute of Biology, Eötvös Loránd University, Budapest, Hungary

[4] Human Brain Tissue Bank, Semmelweis University, Budapest, Hungary

[5] MTA-SE NAP Human Brain Tissue Bank Microdissection Laboratory, Semmelweis University, Budapest, Hungary

[6] Section on Fundamental Neuroscience, National Institute of Mental Health, Bethesda, USA

[#] These authors contributed equally to this work.

Abstract

Recent selective stimulation and ablation of galanin neurons in the preoptic area of the hypothalamus established their critical role in control of maternal behaviors. Here, we identified a group of galanin neurons in the anterior commissural nucleus (ACN), and a distinct group in the medial preoptic area (MPA). Galanin neurons in ACN but not the MPA co-expressed oxytocin. We used immunodetection of phosphorylated STAT5 (pSTAT5), involved in prolactin receptor signal transduction, to evaluate the effects of suckling-induced prolactin release and found that 76 % of galanin cells in ACN, but only 12 % in MPA were prolactin responsive. Nerve terminals containing tuberoinfundibular peptide 39 (TIP39), a neuropeptide that mediates effects of suckling on maternal motivation, were abundant around galanin neurons in both preoptic regions. In the ACN and MPA, 89 and 82 % of galanin neurons received close somatic appositions, with an average of 2.9 and 2.6 per cell, respectively. We observed perisomatic innervation of galanin neurons using correlated light and electron microscopy. The connection was excitatory based on the glutamate content of TIP39 terminals demonstrated by post-embedding immunogold electron

Arpád Dobolyi, dobolyia@caesar.elte.hu.

Electronic supplementary material The online version of this article (doi:10.1007/s00429-016-1246-5) contains supplementary material, which is available to authorized users.

Compliance with ethical standards

Conflict of interest The authors declare that they have no conflict of interest.

microscopy. Injection of the anterograde tracer biotinylated dextran amine into the TIP39-expressing posterior intralaminar complex of the thalamus (PIL) demonstrated that preoptic TIP39 fibers originate in the PIL, which is activated by suckling. Thus, galanin neurons in the preoptic area of mother rats are innervated by an excitatory neuronal pathway that conveys suckling-related information. In turn, they can be topographically and neurochemically divided into two distinct cell groups, of which only one is affected by prolactin.

Keywords

Maternal behavior; Rat dams; Suckling; Prolactin; Oxytocin; Innervation; Preoptic area of hypothalamus

Introduction

It has long been assumed that the preoptic area of the hypothalamus plays a pivotal role in the control of maternal motivation as maternal responsiveness disappears following its bilateral lesion (Numan et al. 1977; Olazabal et al. 2002). In addition, preoptic neurons are activated in mother rats in response to pup exposure (Brunton and Russell 2008; Stern and Lonstein 2001). Galanin is a neuropeptide synthesized in a variety of brain regions, including the preoptic area (Hokfelt et al. 1999; Lang et al. 2007). It has been assumed that preoptic galanin neurons are involved in the control of maternal responsiveness (Bridges 2015). Indeed, a recent breakthrough in the field identified galanin neurons as a major constituent of the neuronal circuitry that regulates maternal behavior in the preoptic area (Wu et al. 2014). A major portion of preoptic area neurons with parenting-induced c-fos were shown to contain galanin. Selective ablation of these neurons resulted in cessation of parental behavior and emergence of pup-directed aggression. In turn, selective optogenetic activation of preoptic galanin neurons resulted in immediate maternal care of pups (Wu et al. 2014). Therefore, the so-far unknown inputs that activate preoptic area galanin neurons have become a major issue in the field (Dobolyi et al. 2014). We aimed to characterize preoptic galanin cells in the rat, including their possible activation by prolactin and neuronal inputs. Since co-localization between galanin and oxytocin has previously been reported in the paraventricular and supraoptic nuclei (Landry et al. 1997), we addressed whether galanin cells in the preoptic area contain oxytocin, a neuropeptide also known to be involved in the control of maternal responsiveness (Bosch and Neumann 2012). Next, we investigated the potential activation of galanin neurons by prolactin. Prolactin is released in large quantities from the pituitary of dams in response to suckling (Neville 2006). Prolactin has been demonstrated to affect maternal motivation (Bridges et al. 1990; Grattan and Kokay 2008); therefore, maternally involved preoptic galanin neurons are its potential targets. Prolactin signal transduction is mediated by STAT5, which is phosphorylated by JAK2 adaptor proteins following the binding of prolactin to its receptor (Martin-Perez et al. 2015). An antibody against the phosphorylated form of STAT5 (pSTAT5) was developed relatively recently. This allowed the immunohistochemical identification of prolactin responsive neurons, and the demonstration that their distribution was very similar to that of the prolactin receptor (Brown et al. 2010). Subsequent studies revealed that a number of neurons in the preoptic area of mother rats become pSTAT5-positive in response to

intracerebroventricular and systemic prolactin injection (Sapsford et al. 2012). These studies demonstrate that increases in preoptic area pSTAT5 are a good indicator of prolactin receptor activation. Thus, we investigated in the present study whether pSTAT5 accumulates in galanin neurons in mother rats in response to suckling. Apart from hormonal effects, preoptic galanin neurons can also be influenced by direct neuronal inputs that convey suckling-related information. We recently characterized an ascending neuronal pathway that is activated by pup exposure (Cservenak et al. 2010). Tuberoinfundibular peptide 39 (TIP39)-expressing neurons in the posterior intralaminar complex of the thalamus (PIL) express the immediate early gene product c-Fos in response to suckling, and their synthesis of TIP39 is also markedly elevated in rat dams. Evidence suggests that TIP39-expressing neurons regulate prolactin release via their projections to the arcuate nucleus (Cservenak et al. 2010; Dobolyi et al. 2010). TIP39, a neuropeptide originally purified from the hypothalamus (Usdin et al. 1999), may also contribute to the control of maternal motivation (Cservenak et al. 2013). Therefore, we examined the possible connection between TIP39 and preoptic galanin neurons by comparing their topographical distributions. Subsequently, using electron microscopy, we addressed whether galanin neurons in the preoptic area are innervated by TIP39 terminals in mother rats, and if the TIP39 synapses are glutamatergic. Finally, the anterograde tracer biotinylated dextran amine was injected into the posterior thalamus, where a group of TIP39 neurons are located to determine if these cells are the origin of TIP39-containing terminals in the preoptic area.

Materials and methods

Animals

This study was approved by Semmelweis University, Budapest, Animal Examination Ethical Council of the Animal Protection Advisory Board. Procedures involving rats were carried out in accordance with the Hungarian Ministry of Agriculture's Animal Hygiene and Food Control Department guidelines for experimental protocols and with EU Directive 2010/63/EU for animal experiments.

A total of 36 mother rats (Wistar; Charles Rivers Laboratories, Hungary) were used (2 for galanin in situ hybridization, 5 for describing galanin-immunoreactive neurons and their oxytocin content, 15 for detecting and quantifying pSTAT5, 5 for the analysis of TIP39 in relation to galanin neurons, 4 for electron microscopy, and 5 for anterograde tracer studies). All animals were 110–140-days-old when killed. Animals were kept under the standard laboratory conditions with 12-h light, 12-h dark periods (lights on at 6.00 AM), and supplied with food and drinking water ad libitum. Pregnant and mother rats were housed individually in standard cages (41 × 22 × 19 cm). Mothers who delivered fewer than eight pups or whose pups died were excluded from the study. The number of pups was adjusted to eight within 2 days of delivery. Experimental manipulations and perfusions of mothers were performed between 10–12 days after delivery. For perfusions and dissections, rats were anesthetized with an intramuscular injection of anesthetic mix containing 0.2 ml/300 g body weight ketamine (100 mg/ml) and 0.2 ml/300 g body weight xylazine (20 mg/ml).

In situ hybridization histochemistry for galanin

Brains of five primiparous female rats were dissected and frozen at 9 days post-partum. In situ hybridization histo-chemistry was performed, as described previously (Dobolyi et al. 2002). Briefly, serial coronal sections (12 μm) were cut, immediately mounted on positively charged slides (Superfrost Plus, Fisher Scientific, Pittsburgh, PA, USA), dried, and stored at −80 °C until use. A 253 bp long region of the rat galanin cDNA sequence (NCBI Reference Sequence: NM_033237.1) was PCR amplified using the following primers: ATGCCATTGACAACCACAGA and CAGTGGGTGTGGTCTCAGGA. The PCR product was subcloned into a TOPO TA vector (Life Technologies) containing a T7 RNA polymerase recognition site. The T7 promoter was used to generate [^{35}S]UTP-labeled ribo-probes, with a MAXIscript transcription kit (Ambion, Austin, TX, USA).

Tissue was prepared using an mRNA-locator Kit (Ambion) according to manufacturer's instructions. For hybridization, we used 80 μl hybridization buffer and 1 million DPM of labeled probe per slide. Washing procedures included a 30 min incubation in RNase A, followed by decreasing concentrations of sodium citrate buffer (pH 7.4) at room temperature, and then at 65 °C. After drying, slides were dipped in NTB nuclear track emulsion (Eastman Kodak, Rochester, NY, USA), stored for 3 weeks at 4 °C for autoradiography, developed with Kodak Dektol developer, fixed with Kodak fixer, counterstained with Giemsa, dehydrated, and coverslipped with Cytoseal 60 (Stephens Scientific, Riverdale, NJ, USA).

Tissue collection for light microscopy

Rats were deeply anesthetized and perfused transcardially with 150 ml saline followed by 300 ml of ice-cold 4 % paraformaldehyde prepared in PB. Brains were removed and post-fixed in 4 % paraformaldehyde for 24 h and then transferred to PB containing 20 % sucrose for 2 days. Serial coronal sections were cut at 50 μm on a sliding microtome between 1.0 and −15.0 mm bregma levels. Sections were collected in PB containing 0.05 % sodium azide and stored at 4 °C.

Microscopy and image processing

Sections were examined using an Olympus BX60 light microscope equipped with fluorescent epi-illumination and a dark-field condenser. Images were captured at 2048 × 2048 pixel resolution with a SPOT Xplorer digital CCD camera (Diagnostic Instruments, Sterling Heights, MI, USA) using 4–40× objectives. Confocal images were acquired with a Nikon Eclipse E800 confocal microscope equipped with a BioRad Radiance 2100 Laser Scanning System using 20–60× objectives at an optical thickness of 1–3 μm. Images were adjusted using the “levels” and “sharpness” commands in Adobe Photoshop CS 8.0. Full resolution of the images was maintained until the final versions, which were adjusted to a resolution of 300 dpi.

Galanin immunohistochemistry

Every fourth free-floating section of five mother rats was immunolabeled for galanin with tyramide amplification fluorescent labeling using a mouse anti-galanin primary antiserum (1:100; catalogue number: orb10685, Biorbyt, Cambridge, UK). For antigen retrieval, the

sections were first incubated in citrate buffer (10 mM sodium citrate, pH 6.0) at 70 °C for 1 h. Then, the sections were incubated in Triton X-100 (0.3 %) containing bovine serum albumin (3 %). Subsequently, primary antiserum was applied for 1 day, then biotin-conjugated donkey anti-mouse secondary antibody at 1:1000 (Jackson ImmunoResearch, West Grove, PA, USA) for 1 h, and then avidin–biotinperoxidase complex (ABC; Vector Laboratories, Burlingame, CA, USA) for 1 h. Subsequently, the sections were incubated in FITC-tyramide (1:3000) and 0.003 % hydrogen peroxide in Tris hydrochloride buffer (0.05 M, pH 8.0) for 6 min, mounted, dried, and coverslipped in antifade medium (Prolong Antifade Kit; Molecular Probes, Eugene, OR, USA).

Double labeling of galanin and oxytocin

One set of every fourth free-floating section from the five rat dams used for single-labeling of galanin was used for double labeling of galanin and oxytocin. First, galanin was immunolabeled using FITC-tyramide amplification immunofluorescence, as described above. Sections were then incubated in citrate buffer at 70 °C for 1 h, and then placed in mouse anti-oxytocin primary antiserum (1:1000; catalogue number: ab78364, Abcam, Cambridge, UK) for 24 h at room temperature and visualized with Alexa Fluor 594 donkey anti-mouse IgG secondary antibody (Thermo Fisher Scientific, Waltham, MA, USA) for 1 h. Subsequently, the sections were mounted, dried, and cover-slipped in antifade medium (Prolong Antifade Kit; Molecular Probes).

After identifying the preoptic sections with the most galanin-ir neurons in the ACN and the MPA in each of the five animals double labeled for galanin and oxytocin, we counted all galanin-ir neurons with an identifiable cell nucleus and all double-labeled cells. Counts were obtained using an Olympus BX60 light microscope with a 20× objective, fluorescent epi-illumination, and a filter that allows for simultaneous green and red visualization.

Measurement of prolactin responsiveness with pSTAT5 immunohistochemistry

Pup exposure of mother rats—Rat dams ($n = 15$) were deprived of pups on post-partum day 8–9 at 13:00. During separation, the litter was held together in a cage that was kept warm by a lamp. The following day at 9:00, pups were returned to the cages of nine mother rats. All nine mothers accepted the pups and suckling started within 5 min. Three of the mothers were perfused 30 min after being reunited with the litter. An additional six mothers were perfused 2 h after their pups were returned to them. Control dams ($n = 6$) were not united with their litters and were killed 21–22 h after the pups had been removed. All animals were perfused as described above and processed for pSTAT5 immunohistochemistry.

Immunolabeling of pSTAT5—One set of every fourth free-floating section from the 15 rat dams used for the prolactin sensitivity study was immunolabeled for pSTAT5 as described for galanin immunolabeling except that rabbit anti-pSTAT5 primary antiserum (1:150; catalogue number: 9351, Cell Signaling Technology Inc., Boston, MA, USA) was used for 48 h at room temperature followed by anti-rabbit secondary antibody at 1:1000 (Jackson ImmunoResearch) for 1 h. After the subsequent application of ABC reagent (Vector Laboratories) for 2 h, the labeling was visualized by incubation in 0.02 % 3,3-

diaminobenzidine (DAB; Sigma), 0.08 % nickel (II) sulfate, and 0.001 % hydrogen peroxide in PB for 4 min. Sections were then mounted, dehydrated, and coverslipped with Cytoseal 60 (Stephens Scientific).

Double immunolabeling of pSTAT5 and galanin—One set of every fourth free-floating section from the 15 rat dams used for single-labeling of pSTAT5 was immunolabeled for pSTAT5 and galanin. Sections were first labeled for galanin using FITC-tyramide amplification immunofluorescence, as described above. Sections were then placed in rabbit anti-pSTAT5 primary antiserum (1:50; Cell Signaling Technology Inc.) for 48 h at room temperature and visualized with Alexa Fluor 594 donkey anti-rabbit secondary antibody (Thermo Fisher Scientific), as described above.

Analysis of double immunolabeling for pSTAT5 and galanin—After identifying the preoptic sections with the most galanin-ir neurons in the ACN and the MPA in each of the 12 animals double labeled for galanin and pSTAT5, we counted all galanin-ir neurons with an identifiable cell nucleus and all double-labeled cells. Counts were obtained using an Olympus BX60 light microscope with a 20× objective, fluorescent epi-illumination, and a filter that allows for simultaneous green and red visualization.

Innervation of galanin neurons by TIP39 terminals

Fluorescent double labeling of TIP39 and galanin—Brain sections of five mother rats were processed for double labeling with TIP39 and galanin. Every fourth free-floating section was first stained for TIP39 using FITC-tyramide amplification fluorescent immunocytochemistry. An affinity-purified antiserum from a rabbit immunized with rat TIP39, which can be absorbed with synthetic TIP39 (Dobolyi et al. 2002), and labels cell bodies with the same distribution as observed by in situ hybridization histochemistry (Dobolyi et al. 2006a, b), was used as primary antiserum. This antiserum (1:3000) was applied for 48 h at room temperature, followed by incubation of the sections in biotinylated donkey anti-rabbit secondary antibody (1:1000; Jackson ImmunoResearch), then in ABC complex (1:500; Vector Laboratories) for 2 h. Sections were subsequently incubated with FITC-tyramide (1:8000) and H_2O_2 in Tris hydrochloride buffer (0.1 M, pH 8.0) for 6 min. Subsequently, mouse anti-galanin antiserum (1:50) was applied as described above followed by Alex-a594 donkey anti-mouse IgG secondary antibody (Thermo Fisher Scientific). Sections were then mounted, dried, and coverslipped as described above.

The analysis of TIP39 innervation of preoptic galanin neurons—Sections double labeled for TIP39 and galanin from three mothers were used for the analysis. There were 60 galaninir neurons analyzed in the ACN and 60 galanin-ir neurons in the MPA. Analysis was performed on serial confocal images collected at an optical thickness of 1 μm. The number of close appositions on different *z* levels belonging to the same cell was summed.

Electron microscopy

Unless otherwise stated, all reagents and materials used for electron microscopic (EM) studies were obtained from Sigma-Aldrich (St. Louis, MO, USA). All experimental

procedures for EM except low-temperature embedding were carried out at room temperature.

Pre-embedding EM immunohistochemistry—Two rats were deeply anesthetized and perfused through the heart with saline for 30 s followed by 500 ml of fixative for 20 min (25 ml/min) made-up of 4 % formaldehyde (Merck) (freshly depolymerized from paraformaldehyde), 0.05 % glutaraldehyde (EM grade), and 0.2 % picric acid in PB. After perfusion, the brains were removed from the skull and washed extensively in PB. 50 lm-thick sections were cut with a vibratome, washed in Tris buffer (0.05 M; pH 7.6) with 0.9 % sodium chloride (TBS), cryoprotected in 30 % sucrose in TBS overnight, and freeze-thawed over liquid nitrogen for three times. After washes and treatment with 1 % hydrogen peroxide, the sections were processed for immunostaining using the following protocol: quenching in 50–50 mM ammonium chloride and glycine dissolved in TBS for 30 min; blocking 2 % BSA for 1 h; anti-TIP39 antiserum (1:3000) diluted in 0.5 % BSA-TBS for 48 h; biotin-conjugated goat anti-rabbit secondary antibody at 1:500 (Vector Laboratories); and ABC at 1:500 (Vector Laboratories). The immunoperoxidase reaction was developed with nickel-intensified 3,3-diaminobenzidine (Ni-DAB) as described above (black reaction product). After the first reaction, the sections were processed for a second immunostaining. The same protocol was carried out except that the primary antiserum was mouse anti-galanin antibody (1:200; catalogue number: orb10685, Biorbyt, Cambridge, UK), followed by biotin-conjugated goat anti-mouse secondary antibody at 1:500 (Vector Laboratories). The second immunoperoxidase reaction was developed with DAB (brown reaction product). All sections were post-fixed in 0.5 % OsO_4 containing 3.5 % glucose in 0.1 M Na-cacodylate to preserve DAB–Ni-DAB color differences. This was followed by en bloc staining with half-saturated aqueous uranyl acetate, dehydration in a series of ethanol at increasing concentrations and acetonitrile, and then embedding in Durcupan (ACM; Fluka). Sections were embedded on slides and cured for 48 h at 60 °C. Small pieces from the MPA-containing galaninimmunoreactive cells were reembedded and resectioned at 70 nm. Section were collected on pioloform coated single slot copper grids and stained with lead citrate for 1 min.

Tissue preparation and low-temperature embedding for electron microscopic immunogold labeling—Two mother rats were perfused through the heart with saline for 30 s followed by fixative containing 2 % formaldehyde (freshly depolymerized from paraformaldehyde) and 0.5 % glutaraldehyde dissolved in PB for 20 min. After this relatively strong fixation, which is necessary to preserve glutamate in the tissue (Ottersen 1989), the brains were perfused again with saline for 10 min to avoid overfixation. Then, the brains were removed from the skull and sectioned at 50 μm on vibratome. Brain sections containing the MPA were processed for low-temperature embedding, as described before (Berryman and Rodewald 1990). Briefly, free aldehydes were quenched with a solution that contained 50 mM ammonium chloride and 50 mM glycine dissolved in TBS. Then, blocks were washed three times in maleate buffer (0.05 M, pH 5.5) before post-fixation in 1 % uranyl acetate dissolved in maleate buffer for 180 min in the dark. This was followed by three washes in maleate buffer. Subsequently, blocks were dehydrated in graded series of acetone while progressively lowering the temperature. Samples were then infiltrated with

pure LR White alone for 12 h, at −20 °C followed by pure LR White containing 2 % benzoyl peroxide as a catalyst for 3 h, at −20 °C. Curing was performed with a homemade UV chamber using two DL-103 2 × 6 W UV lamps for 60 h at −20 °C.

Post-embedding immunogold labeling for TIP39 and glutamate—Small pieces from the MPA were reembedded and resectioned at 70 nm. Sections were collected on formvar-coated single slot nickel grids allowing immunoreaction on one side of the sections. To demonstrate the presence of TIP39 and glutamate in the same terminal only, two sections were collected on one grid. Four grids carrying consecutive serial sections were immunolabeled; therefore, terminals were present on multiple sections and could be treated with different antibody solutions on adjacent sections. All immunoreactions were carried out on humidified parafilm-coated 96-well plates. TBS was used for all washes and dilutions. Briefly, the following procedure was carried out: (1) 5 % hydrogen peroxide for 3 min; (2) wash in double distilled water (biDW; (3) 1 % sodium borohydride and 50 mM glycine dissolved in TBS for 2 min; (4) wash in TBS; (5) 1 % BSA for TIP39 and 1 % ovalbumin for glutamate reaction for 30 min; (6) rabbit anti-TIP39 antiserum in 1:100 or rabbit anti-glutamate antibody (Code no: 13, gift from Prof. Peter Somogyi, MRC BNDU, Oxford, UK) in 1:2000 dilution in 0.5 % ovalbumin-TBS containing 0.05 % sodium azide for 12–18 h; (7) washes in 0.5 % ovalbumin-TBS; (8) 10 nm gold-conjugated goat anti-rabbit secondary antibody 1:50 in TBS with 1 % ovalbumin for 4 h; (9) wash in TBS; (10) 2 % glutaraldehyde in TBS for 10 min; (11) wash in biDW; (12) air drying; (13) staining in half-saturated aqueous uranyl acetate for 30 min followed by lead citrate for 30 s; and (14) air drying.

Double-immunogold labeling for glutamate and GABA—Ultrathin sections (70 nm) were collected on formvar-coated 100-mesh nickel grids. The first immunoreaction against glutamate was carried out as described above except, that 18 nm gold bead-conjugated donkey anti-rabbit secondary antibody (1:50, Jackson ImmunoResearch) was used. Since both glutamate and GABA antisera were produced in rabbits, after the first immunoreaction remaining free immunoglobulin molecules were inactivated using the formaldehyde vapor treatment (Phend et al. 1992; Wang and Larsson 1985). Briefly, after air drying, the grids were placed in a plastic Petri dish with section side up, containing paraformaldehyde crystals and placed in an oven for 60 min at 80 °C. After incubation in TBS, grids were treated with rabbit anti-GABA antibody (1:10,000, catalogue number A2052, Sigma-Aldrich). After several washes in 0.5 % ovalbumin-TBS, the sections were incubated in 10 nm gold bead-conjugated goat anti-rabbit secondary antibody (1:50 in TBS with 0.5 % ovalbumin) for 4 h. The sections were rinsed in TBS, and the immune complexes were fixed with 2 % glutaraldehyde for 10 min. Then the sections were air dried and counterstained with 0.5 % osmium tetroxide and lead citrate for 20 min and 30 s, respectively.

Electron microscopic image acquisition and processing—For correlated light and electron microscopy, candidate galanin-immunoreactive cells were photographed with a light microscope before reembedding. During ultrathin sectioning the block face was checked repeatedly to reach the appropriate depth containing potential synaptic contacts. In the EM, putative glutamatergic (also called asymmetrical) and GABA/glycinergic (also

called symmetrical) synaptic junctions were identified on the basis of their fine structure. Briefly, asymmetrical synapses possess a thick post-synaptic density, whereas symmetrical synapses are characterized by a thin post-synaptic density. The same criteria were used in the case of post-embedding TIP39, glutamate, and GABA immunogold labeling. In the latter, who used low-temperature embedded materials, the contrast was low due to the lack of osmium tetroxide treatment. In turn, post-synaptic specializations were more apparent, which allowed us to reliably differentiate presumed excitatory and inhibitory terminals.

For the identification of TIP39 and glutamate, special criteria were applied as glutamate immunogold detection requires high glutaraldehyde fixation (Ottersen et al. 1990), which resulted in weak TIP39 immunoreactivity. Therefore, only terminals that were positive for TIP39 on two adjacent sections were further analyzed for glutamate-like immunoreactivity. Using this method, we could differentiate low, but specific TIP39 immunoreactivity from background labeling.

Electron micrographs were taken by a side-mounted Morada CCD camera (Olympus Soft Imaging Solutions) connected to a JEOL 1011 or with a Gatan UltraScan 1000 CCD camera fitted to a Philips CM100 electron microscope. Due to the low contrast of the specimen, brightness and contrast were adjusted when necessary in the whole digital images of immunogold labeling using Adobe Photoshop CS2 (Adobe Systems).

Quantitation of glutamate and GABA double labeling—In the Glu/GABA double-immunogold labeling, synaptic terminals (39 asymmetric and 22 symmetric) with clearly visible synaptic specialization were photographed and their area was determined with iTEM software (iTEM Software, Irvine, CA, USA) using the interpolated polygon algorithm. In the EM, asymmetric and symmetric synapses were identified on the basis of their fine structure as described above. Gold particle densities representing glutamate and GABA over terminals were counted. Glutamate and GABA ratios were calculated for both symmetric and asymmetric synapses. Data were analyzed using the Mann–Whitney U test.

Anterograde tracing

Injection of anterograde tracer—The anterograde tracer biotinylated dextran amine (BDA; 10,000 MW, Molecular Probes) was targeted to the PIL ($n = 5$). The relation of the injection site to the position of TIP39 neurons was verified by double labeling. Some of the misplaced injections were used as controls. For stereotaxic injections, rats were positioned in a stereotaxic apparatus with the incisor bar set at −3.3 mm. Holes of about 2-mm diameter were drilled into the skull above the target coordinates. Glass micropipettes of 15–20-μm internal diameter were filled with 10 % BDA dissolved in PB and lowered to the following stereotaxic coordinates (Paxinos and Watson 2007): AP = −5.2 mm from bregma, $L = 2.6$ mm from the midline, $V = 6.4$ mm from the surface of the dura mater. Once the pipette was in place, the BDA was injected by iontophoresis using a constant current source (51413 Precision Current Source, Stoelting, Wood Dale, IL, USA) that delivered a current of +6 μA, which pulsed for 7 s on and 7 s off for 15 min. Then, the pipette was left in place for 10 min with no current and withdrawn under negative current. After tracer injections, the animals were allowed to survive for 7 days.

Visualization of BDA—Sections from rat brains injected with BDA were stained using biotin-tyramide amplification immunofluorescent labeling. Every fourth free-floating section was pretreated in PB-containing 0.5 % Triton X-100 for 1 h and then incubated in ABC (Vector Laboratories) at 1:300 for 2 h. Next, sections were placed in biotin-tyramide solution (1:1000) containing 0.003 % hydrogen peroxide for 20 min. Then, a second ABC incubation was conducted at 1:1000 for 1 h. Finally, the reaction product was visualized by incubation in 0.02 % DAB (Sigma), 0.08 % nickel (II) sulfate, and 0.003 % hydrogen peroxide in PB. After washes, the sections were mounted, dehydrated, and coverslipped with Cytoseal 60 (Stephens Scientific), as described above.

Double labeling of BDA and TIP39—Brain sections of animals injected with BDA were processed for BDA-TIP39 double labeling. First, BDA visualization was performed as described above, but using Alexa Fluor 594-tyramide amplification instead of DAB reaction. Subsequently, TIP39 was visualized by incubating the sections in anti-TIP39 primary antiserum for 48 h, as described above, followed by incubation in Alexa Fluor 488 anti-rabbit secondary antibody (Thermo Fisher Scientific) at 1:500 for 2 h. Finally, sections were mounted and coverslipped, as described above for fluorescent labeling.

Results

Location of galanin neurons in the preoptic area

The distributions of galanin neurons identified either by their mRNA expression, using radioactive in situ hybridization histochemistry, or by their protein content, detected by immunolabeling were very similar in the pre-optic area of mother rats. There was a high density of galanin neurons in the anterior commissural nucleus (ACN), which is situated in the medial part and dorsal part of the preoptic area (Fig. 1). There were some scattered cells medial to this cell group along the ventricle immediately medial to the ACN. Less densely packed galanin neurons were present ventrolateral to the ACN in a large area within the medial preoptic area (MPA). Other parts of the preoptic area, including the medial preoptic nucleus and the lateral preoptic area, contained only a few scattered galanin neurons except for the ventrolateral preoptic nucleus, which contained a significant number of galanin neurons (Fig. 1).

Oxytocin content of galanin neurons

Oxytocin neurons are present in the preoptic area of the rat as demonstrated by immunolabeling oxytocin. Labeling of sagittal sections also demonstrated that the oxytocin cells in the preoptic area form a population distinct from the major oxytocinergic cell group in the paraventricular nucleus (Supplementary Figure 1). In the ACN, the coronal preoptic sections with the most galanin-ir neurons contained 46 ± 6 galanin-immunoreactive (-ir) cells. The majority of galanin-ir neurons (88 %) also contained oxytocin immunoreactivity (Fig. 1c, d). In turn, most oxytocinir cells in the ACN were galanin-positive (91 %). Thus, the high degree of co-expression suggests that there is an abundant cell group which contains both neuropeptides. However, the subcellular localization of the two peptides was different. Although some co-localization existed, galanin immunoreactivity was associated with granule-like structures, while oxytocin had a more even distribution in the cell bodies

(Fig. 1c, d). In addition, dendrites, including secondary dendrites, contained oxytocin immunoreactivity. In contrast, galanin immunoreactivity was largely confined to the cell bodies, and only the proximal parts of some primary dendrites contained galanin.

In the MPA, the preoptic sections with the most galaninir neurons contained 24 ± 5 galanin-ir neurons. Some double-labeled oxytocin-containing galanin neurons appeared in the caudal part of the MPA, but overall most of these neurons were negative for oxytocin. The percentage of galanin-ir neurons that also expressed oxytocin was 9 %. The presence of single-labeled galanin-ir cells provided evidence that bleed-through did not take place using our double labeling procedures for galanin and oxytocin.

There were only a few pSTAT5-immunoreactive neurons in the preoptic area of rat dams at 24 h after the removal of their litter. These cells were mainly present in the periventricular nucleus while the MPA and the ACN contained only a very few labeled cells (Fig. 2a-2). When the pups were returned to the mother, suckling started within 5 min. It is known that serum prolactin levels are maximal 30 min following the beginning of suckling and then remain high as long as the pups are present (Cservenak et al. 2010; Freeman et al. 2000). Indeed, at 30 min after the beginning of suckling, a number of pSTAT5-ir cells were detectable in the preoptic area. We observed a somewhat higher number of pSTAT5-ir cells at 2 h after the beginning of suckling with the same distribution as after 30 min. Cells-containing pSTAT5 were present in the medial part of the preoptic area, including the ventrally situated medial preoptic nucleus as well as the periventricular nucleus, and the mediodorsal part of the preoptic area, which includes the ACN (Fig. 2a-1). In the section, which contained the most galanin-ir cells in the ACN, we counted 44 ± 8 galanin-ir cells, of which 35 ± 6 were double labeled, that is 79 % of galanin neurons in the ACN contained pSTAT5. In contrast, a very few pSTAT5-ir cells were present in the MPA, where the ventrolateral group of MPA galanin neurons were located. In the section of the MPA, which contained the most galanin-ir cells, we counted 20 ± 4 galanin-ir cells, of which 2.5 ± 1.2 were double labeled, that is 12 % of galanin neurons in the MPA contained pSTAT5 (Fig. 2b, c). Thus, the ratio of pSTAT5-ir (prolactin responsive) cells differed significantly between the two groups of galanin neurons.

Innervation of preoptic galanin neurons

As the major ascending sensory pathway providing suckling-related information to the preoptic area contains the neuropeptide TIP39 (Dobolyi et al. 2014) and galanin neurons are critically important for maternal behaviors (Dulac et al. 2014; Wu et al. 2014), we examined the topographical relationship between TIP39 and galanin. TIP39 fibers are localized in the medial preoptic nucleus, the MPA, and the ventral subdivision of the bed nucleus of the stria terminalis, as well as the ACN. In the MPA and the ACN, TIP39 fibers surrounded galanin-ir neurons (Fig. 3). In fact, a number of TIP39-containing varicosities closely apposed the cell bodies and proximal dendrites of galanin-ir neurons. In the ACN and MPA, 89 and 82 % of galanin neurons received an average of 2.9 and 2.6 close appositions per cell, respectively. Correlated light and electron microscopy proved that TIP39-positive thalamic axons innervate galanin neurons in the MPA (Fig. 4). Galanin-ir somata received multiple

conventional asymmetrical (putative glutamatergic) synapses from TIP39-positive axon terminals.

The synaptic morphology of 17 TIP39-ir boutons was analyzed, and all of them formed asymmetric synapses. Previous immunocytochemical studies using highly specific antibodies against glutamate and GABA showed a precisely correlated relationship between synaptic morphology and transmitter content (Ottersen et al. 1990; Somogyi et al. 1986). Briefly, boutons forming asymmetrical synapses have a high glutamate/GABA immunoreactivity ratio. In contrast, glutamate/GABA immunoreactivity ratios in symmetric (putative GABAergic) terminals are several folds lower than in glutamatergic terminals due to the high efficiency conversion of glutamate into GABA by glutamic acid decarboxylase (GAD) enzymes GAD65 and/or 67 (Broman et al. 2000). Therefore, asymmetric synapses are widely considered as markers of putative glutamatergic boutons. Although glutamate and GABA immunoreactivities have been shown in various hypothalamic nuclei (Decavel and Van den Pol 1990, 1992; Meeker et al. 1993), the simultaneous labeling of the two neurotransmitters in the same material and their relationship to synaptic ultrastructure in the MPA has not yet been reported. Therefore, we performed double-immuno-gold labeling for glutamate and GABA in the same material, and found that, indeed, symmetric and asymmetric synapses formed highly distinct clusters based on the densities of gold particles representing glutamate and GABA immunoreactivities in their boutons (Supplementary Figure 2A, B). Furthermore, the glutamate/GABA ratios differed significantly between the two morphological groups of synapses (Supplementary Figure 2C). These findings also confirmed the specificity of the glutamate antiserum coded Glu13 (Storm-Mathisen et al. 1983) in our procedure.

To obtain direct evidence about the glutamatergic nature of TIP39 terminals, we performed post-embedding immunolabeling of consecutive serial sections for TIP39 and glutamate (Fig. 5). Due to the high glutaraldehyde fixation, which is a prerequisite for the detection of glutamate (Ottersen 1989), the signal for TIP39 immunore-activity was weak, but it was specific, as it was present only in some boutons (Fig. 5a, c), while other structures were devoid of TIP39 immunoreactivity. We also observed the presence of dense core vesicles in TIP39 positive terminals representing the potential storage sites of the neuropeptide. Immunolabeling of adjacent sections for glutamate revealed that boutons shown to be immunoreactive for TIP39 in previous consecutive sections also contain a high density of glutamate immunoreactivity (Fig. 5b, d), which provides direct evidence of the glutamatergic nature of synapses made by TIP39-ir terminals, as previously demonstrated by similar immunogold labeling against glutamate in various brain regions and cell types (Bergersen et al. 2012; Bramham et al. 1990; Didier et al. 2001; Jenstad et al. 2009; Matsubara et al. 1996). Indeed, boutons associated with symmetric (putative GABA/glycinergic) synapses, and some myelinated axons did not exhibit glutamate immunoreactivity (Fig. 5b, d).

The origin of preoptic TIP39 terminals

We injected the anterograde tracer BDA into the PIL to identify the origin of TIP39 fibers in the preoptic area. There were two injections in which the spread of tracer overlapped entirely

or almost entirely with the location of the TIP39 neurons (Fig. 6a) and many TIP39 cells took up the tracer (Fig. 6b). The topographical distribution of BDA-labeled fibers in the preoptic area did not differ in these brains. For example, the arcuate nucleus, which is known to receive TIP39 fibers from the PIL based on the previous retrograde studies (Cservenak et al. 2013), contained BDA fibers. Therefore, the description of the fibers reaching the preoptic area from the PIL is based on the results of these two injections. Injections adjacent to the PIL resulted in labeling patterns markedly different from those following PIL injections suggesting that the projections observed were those of PIL neurons.

The distribution of BDA-labeled fibers in the preoptic area was similar to that of TIP39-ir fibers (Fig. 7a). In fact, most BDA fibers in the preoptic area were double labeled with BDA and TIP39 (Fig. 7b). Other parts of the preoptic area contained low or only a very low density of BDA fibers. The great majority of labeled fibers were always ipsilateral to the injection side, and only a low or very low density of labeled fibers was present contralaterally in the same regions that received massive ipsilateral input (Fig. 7a). The distribution pattern following PIL injections differed considerably from those of non-overlapping control injections.

Discussion

Classification of preoptic galanin neurons

The high degree of similarity between the localizations of galanin neurons determined on the basis of mRNA expression and immunoreactivity argues strongly for the specificity of the galanin labeling. Indeed, we found a generally similar distribution of galanin in the preoptic area to that previously described in male rats (Jakobowitz and Skofitsch 1991). However, we did not observe galanin neurons in the medial preoptic nucleus (MPN), which is in agreement with the previous reports that only males contain galanin neurons in the MPN (Bloch et al. 1998). It is also noteworthy that the distribution of galanin neurons may be different in the rat and mouse, as in the latter species, some parts of the female MPN may also contain galanin cells, albeit in a strain-dependent manner (Mathieson et al. 2000). Some of the preoptic galanin neurons may express gonadotropin-releasing hormone (Rossmanith et al. 1996). However, it has often been reported that the expression of galanin may be conditional, and depend on sex, hormonal background, and other factors in different hypothalamic neurons in various species (Christiansen 2011; Diaz-Cabiale et al. 2014; Garcia-Falgueras et al. 2011; Hammouche and Bennis 2013; Porteous et al. 2011; Tillet et al. 2012; Whitelaw et al. 2012). Therefore, the possibility exists that the difference between the distribution of galanin in rats and mice could be a consequence of conditions apart from the species difference. It is also worth mentioning that a distinct portion of the preoptic area, the ventrolateral preoptic nucleus contains cells that constitutively express galanin. These, however, are not likely to be involved in the control of maternal behaviors, but are known to participate in the control of sleep (Gavrilov et al. 2016). It has also been reported previously that some galanin neurons contain oxytocin. These studies focused on the paraventricular and supraoptic nuclei, which both contain oxytocin neurons that co-express galanin (Meister et al. 1990). The presence of galanin in paraventricular and supraoptic magnocellular oxytocin neurons has also been reported in lactating mother rats (Landry et al. 1997).

Furthermore, the galanin content of oxytocin neurons was reported to decrease on post-partum day 1 and return to the level of non-lactating females by post-partum day 7 (Eriksson et al. 1996). However, the posterior oxytocinergic cells were not investigated in the present study, because only preoptic and not general hypothalamic galanin neurons were strongly implicated in the control of maternal behaviors (Wu et al. 2014). Furthermore, only lesions involving preoptic oxytocin neurons, but not more caudal paraventricular lesions reduced maternal behaviors in mother rats (Insel and Harbaugh 1989) suggesting that the preoptic oxytocin neurons may have specific roles in the control of maternal behaviors exerted by oxytocin (Pedersen et al. 2006; Strathearn et al. 2009).

In the present study, we report that oxytocin neurons in the ACN (anterior commissural nucleus—sometimes also called lateral commissural nucleus)—also contain galanin. Magnocellular neurons in the ACN have been considered as an anterior magnocellular subdivision of the paraventricular nucleus (Hou-Yu et al. 1986; Nylen et al. 2001). However, the ACN is often dismissed as an accessory nucleus during investigation and discussion of the oxytocin system (Briski and Brandt 2000; Knobloch and Grinevich 2014; Powers-Martin et al. 2008), even though 616 oxytocin cells were counted in the ACN which is more than 50 % of the 1174 oxytocin cells of the paraventricular nucleus in the rat (Rhodes et al. 1981), and the morphology as well as the oxytocin content of oxytocin neurons in the ACN were comparable to that in the PVN (Burbach et al. 1987, 2006; Castel and Morris 1988). Surprisingly, even recent studies on the detailed parcellation of the paraventricular nucleus fail to mention a rostral magnocellular subdivision (Simmons and Swanson 2008). Oxytocin neurons in the ACN may have properties different from those in the paraventricular and supraoptic nucleus. Oxytocin appears in the ACN later in ontogeny than in the paraventricular and supraoptic nuclei (Laurent et al. 1989). Estrogen treatment of ovariectomized female rats selectively reduced oxytocin labeling in the ACN (Caldwell et al. 1988), but oxytocin levels in the ACN did not vary across the estrous cycle, in contrast to the paraventricular nucleus (Greer et al. 1986). Indeed, estrogen receptor beta was not detected in the area corresponding to ACN (Laflamme et al. 1998). In addition, p450 aromatase was present in oxytocin cells of the ACN, but not in the two major oxytocin-containing nuclei (El-Emam Dief et al. 2013). In addition, deletion of nitric oxide synthase selectively increased oxytocin expression in the ACN (Nomura et al. 2005). These differences between the oxytocin-containing cells of the ACN and the paraventricular nucleus suggest that their role in the control of maternal responsiveness may also be different.

Hormonal and neuronal inputs to preoptic galanin neurons

Steroid hormones as well as prolactin are important in the induction of maternal behaviors (Bridges 2015). However, the maintenance of maternal responsiveness primarily relies on sensory input from the pups that reaches the preoptic area (Numan and Insel 2003). A particularly important input derives from suckling, which activates brain regions responsible for maternal responsiveness (Li et al. 1999), and also leads to the release of prolactin from the pituitary. Elevated serum prolactin levels have a peak at about 30 min following the beginning of suckling (Freeman et al. 2000). The released prolactin stimulates lactation and may also play a modulatory role in the regulation of post-partum anxiety (Torner et al. 2002). Prolactin can enter the brain at the circumventricular organs and also through the

blood-cerebrospinal fluid barrier via a receptor-mediated transport process (Grattan and Kokay 2008). The prolactin receptor is present in several distinct brain regions, including the medial part of the preoptic area (Mann and Bridges 2002). Therefore, it was not surprising that the adminstration of prolactin into the lateral ventricle or of a higher dose into the blood resulted in the appearance of pSTAT5 in the medial part of the preoptic area (Saps-ford et al. 2012). However, our results are the first to demonstrate that pSTAT5 immunoreactivity also appears in the medial part of the preoptic area following suckling, and its distribution is the same as after exogenous prolactin injection (Sjoeholm et al. 2011) and in continuously lactating dams (Brown et al. 2011), which suggests that prolactin itself caused the phosphorylation of STAT5 following suckling. The presence of pSTAT5 at both 30 min and 2 h following the beginning of suckling might be explained by the continuous presence of detectable level of pSTAT5 in the presence of high prolactin concentration. The appearance of pSTAT5 in galanin neurons suggest that these cells are directly affected by prolactin following suckling. In fact, most galanin neurons in the ACN contained pSTAT5, suggesting that prolactin has a significant effect on members of this cell group, which could contribute to the anxiolytic effect of prolactin during lactation (Torner et al. 2002). In contrast, the majority of the galanin neurons in the MPA were devoid of pSTAT5. While the possibility that a higher concentration of prolactin would affect these cells cannot be excluded, their physiological activation by direct prolactin action is not likely.

Direct neuronal input is another potential route for the activation of galanin cells in mothers. It has been proposed that somatosensory input from the nipples may activate galanin neurons (Bridges 2015). The anatomical pathway conveying this information relays in the posterior intralaminar complex of the thalamus (PIL), where TIP39-expressing neurons demonstrate profound c-fos activation in response to suckling if the pups are allowed physical contact for suckling (Cservenak et al. 2013). The PIL includes the posterior intralaminar thalamic nucleus, the parvicellular subparafascicular nucleus, and some parts of the caudal subdivision of the zona incerta (Dobolyi et al. 2003). The presence of anterograde tracer in the preoptic area following its injection into the PIL suggests that neurons of the PIL can relay suckling information to the preoptic area. These data also confirm previous retrograde tracer studies demonstrating that the medial preoptic area receives projections from the area corresponding to the PIL (Simerly and Swanson 1986). Furthermore, the finding that TIP39 terminals synapse on the cell bodies and proximal dendrites of galanin neurons, the first ever demonstration that TIP39 terminals form conventional synapses, suggest an efficient innervation of galanin neurons by TIP39-containing fibers. The glutamatergic nature of TIP39 terminals shown in the present study by both correlated light and electron microscopic observations and post-embedding immunogold electron microscopy of serial sections suggests an excitatory connection between TIP39 terminals and galaninergic neurons. Thus, while other neuronal inputs to the galanin neurons may also convey information about pup interaction, TIP39 terminals are likely to play an important role in this process. TIP39 itself may modulate the synaptic information transfer as the receptor for TIP39, parathyroid hormone 2 receptor (PTH2R) is abundant in the preoptic area (Dobolyi et al. 2006a, b). Since the PTH2R is also excitatory (Dobolyi et al. 2010), we conclude that the activity of galanin neurons is likely increased by the input from the PIL. This regulation may supplement another related function of TIP39 neurons in the PIL. Anterograde tracer

delivery to the area corresponding to our injection site labeled fibers in the arcuate nucleus, and that projection was confirmed by a retrograde study (Szabo et al. 2010). Double labeling revealed that subpopulations of the neurons projecting to the arcuate nucleus contained TIP39 (Szabo et al. 2010). Indeed, an antagonist of the PTH2R blocked suckling induced prolactin release in rat dams (Cservenak et al. 2010). Thus, the possibility exists that the same neurons convey suckling information to the arcuate nucleus to evoke prolactin release and also to the preoptic area to elicit maternal behavior (Dobolyi 2011).

Possible roles of preoptic galanin neurons and their inputs in maternal responsiveness

The dominant role of the preoptic area in the control of maternal responsiveness has been established primarily on the basis of activation and lesion studies. Indeed, c-fos activation is induced in the preoptic area of mother rats in response to pup exposure (Stack and Numan 2000), while the lesion of the preoptic area disrupts maternal behaviors (Numan et al. 1977; Olazabal et al. 2002). Recently, pre-optic galanin neurons were shown to express c-fos in response to pup exposure, while their specific lesion using a virus to express diphtheria toxin in galanin neurons resulted in the disappearance of maternal behaviors in mice (Wu et al. 2014). In turn, optogenetic stimulation of pre-optic galanin neurons led even male mice to perform nurturing behaviors (Wu et al. 2014). These results indicate that galanin neurons play critically important roles in the control of maternal behaviors in mice and, possibly, also in the rat (Dulac et al. 2014). In turn, our results suggest that different populations of galanin neurons exist in the pre-optic area that may participate in potentially different specific maternal functions. While the preoptic maternal circuitry is not well known, its outputs were divided into two major components: the activation of reward centers, including the ventral tegmental area and the nucleus accumbens, and the inhibition of pup aversion through projections to the amygdala and the periaqueductal gray (Brunton and Russell 2008). Although widespread projections from the preoptic area to these brain sites have been described (Simerly and Swanson 1988), the targets of the different groups of galanin neurons are not known. The role of galanin itself is another interesting question. While it was shown that galanin injected into the medial preoptic nucleus facilitated sexual behaviors in female rats (Bloch et al. 1996), a direct effect of galanin on maternal behaviors has not been reported. In turn, the increase of oxytocin levels specifically in the ACN during lactation (Brooks et al. 1990) suggests maternal function of the ACN, as well as oxytocin potentially released from neurons of this nucleus. Since oxytocin is generally known to promote maternal behaviors (Bosch and Neumann 2012) and specifically, its local injection into the preoptic area evokes this effect (Pedersen et al. 1994), oxytocin is a candidate to mediate the maternal actions of the stimulation of ACN galanin neurons. Galanin could modulate these oxytocin effects, as it was shown to affect oxytocin release from magnocellular oxytocin neurons (Ciosek and Drobnik 2013).

The afferent neuronal connections of the preoptic area have been known for a long time (Simerly and Swanson 1986), yet the inputs important for maternal responsiveness remain to be elucidated. In general, olfactory and somatosensory inputs derived from the pups may be the most important for rodent mothers (Dobolyi et al. 2014). Olfactory input likely arrives at the preoptic area from the amygdala (Fleming and Walsh 1994), while suckling-derived somatosensory information reaches the preoptic area through the posterior thalamus

(Cservenak et al. 2013). Our findings that neurons of the PIL project to preoptic galanin neurons and innervate them suggest that galanin neurons receive suckling-derived information, which is likely to be important for their activity and actions. A specific role of TIP39 in this projection can be hypothesized based on previous results showing that local blockade of TIP39's receptor in the preoptic area reduced maternal motivation measured by a conditioned place preference test (Cservenak et al. 2013). The action of TIP39 on galanin neurons is clearly a candidate for the effect of TIP39 on maternal motivation. However, the maintenance of proper maternal responsiveness may also require prolactin hormonal input to the preoptic area (Stern and Lonstein 2001). Indeed, the appearance of pSTAT5 in preoptic neurons suggests that they are directly affected by prolactin. The marked difference between the induction of pSTAT5 in the dorsomedial and ventromedial galanin cell groups implies that only the former cell group is significantly affected by prolactin. While prolactin promotes a variety of different maternal behaviors (Larsen and Grattan 2012), the specific function of prolactin action on galanin neurons in the ACN remains to be established.

In conclusion, two different subgroups of galanin neurons exist in the preoptic area and potentially play a part in the regulation of maternal responsiveness: one mainly located in the anterior commissural nucleus (ACN) and the other in the medial preoptic area. While only the dorsomedially located galanin cells in the ACN contain oxytocin, cell bodies and proximal dendrites of galanin neurons in both cell groups receive synaptic innervation from ascending TIP39-containing projections that convey information on suckling. These projections arise from the posterior intralaminar complex of the thalamus and are glutamatergic. In turn, only the dorsomedial group of galanin cells in the ACN is significantly affected by prolactin. The results also support the idea that galanin neurons in the preoptic area of mother rats are involved in the control of maternal responsiveness.

Supplementary Material

Refer to Web version on PubMed Central for supplementary material.

Acknowledgments

Grant support was provided by HAS Postdoctoral Research Fellowship Program for MCs, OTKA K100319, OTKA K116538 and KTIA_NAP_B_13-2-2014-0004 Program for AD, and NIMH IRP for TBU. The technical assistance of Nikolett Hanák and Szilvia Deák is also acknowledged. The authors also thank Cintia K Finszter for technical contribution to pSTAT5 immunohistochemistry.

References

Bergersen LH, Morland C, Ormel L, Rinholm JE, Larsson M, Wold JF, Roe AT, Stranna A, Santello M, Bouvier D, Ottersen OP, Volterra A, Gundersen V. Immunogold detection of L-glutamate and D-serine in small synaptic-like microvesicles in adult hippocampal astrocytes. Cereb Cortex. 2012; 22:1690–1697. [PubMed: 21914633]

Berryman MA, Rodewald RD. An enhanced method for post-embedding immunocytochemical staining which preserves cell membranes. J Histochem Cytochem. 1990; 38:159–170. [PubMed: 1688894]

Bloch GJ, Butler PC, Kohlert JG. Galanin microinjected into the medial preoptic nucleus facilitates female- and male-typical sexual behaviors in the female rat. Physiol Behav. 1996; 59:1147–1154. [PubMed: 8737905]

Bloch GJ, Butler PC, Eckersell CB, Mills RH. Gonadal steroid-dependent GAL-IR cells within the medial preoptic nucleus (MPN) and the stimulatory effects of GAL within the MPN on sexual behaviors. Ann N Y Acad Sci. 1998; 863:188–205. [PubMed: 9928171]

Bosch OJ, Neumann ID. Both oxytocin and vasopressin are mediators of maternal care and aggression in rodents: from central release to sites of action. Horm Behav. 2012; 61:293–303. [PubMed: 22100184]

Bramham CR, Torp R, Zhang N, Storm-Mathisen J, Ottersen OP. Distribution of glutamate-like immunoreactivity in excitatory hippocampal pathways: a semiquantitative electron microscopic study in rats. Neuroscience. 1990; 39:405–417. [PubMed: 2087264]

Bridges RS. Neuroendocrine regulation of maternal behavior. Front Neuroendocrinol. 2015; 36:178–196. [PubMed: 25500107]

Bridges RS, Numan M, Ronsheim PM, Mann PE, Lupini CE. Central prolactin infusions stimulate maternal behavior in steroid-treated, nulliparous female rats. Proc Natl Acad Sci USA. 1990; 87:8003–8007. [PubMed: 2236014]

Briski KP, Brandt JA. Oxytocin and vasopressin neurones in principal and accessory hypothalamic magnocellular structures express Fos-immunoreactivity in response to acute glucose deprivation. J Neuroendocrinol. 2000; 12:409–414. [PubMed: 10792579]

Broman J, Hassel B, Rinvik E, Ottersen OP. Biochemistry and anatomy of transmitter glutamate. Handb Chem Neuroanat. 2000; 18:1–44.

Brooks PJ, Lund PK, Stumpf WE, Pedersen CA. Oxytocin messenger ribonucleic acid levels in the medial preoptic area are increased during lactation. J Neuroendocrinol. 1990; 2:621–626. [PubMed: 19215397]

Brown RS, Kokay IC, Herbison AE, Grattan DR. Distribution of prolactin-responsive neurons in the mouse forebrain. J Comp Neurol. 2010; 518:92–102. [PubMed: 19882722]

Brown RS, Herbison AE, Grattan DR. Differential changes in responses of hypothalamic and brainstem neuronal populations to prolactin during lactation in the mouse. Biol Reprod. 2011; 84:826–836. [PubMed: 21178171]

Brunton PJ, Russell JA. The expectant brain: adapting for motherhood. Nat Rev Neurosci. 2008; 9:11–25. [PubMed: 18073776]

Burbach JP, Voorhuis TA, van Tol HH, Ivell R. In situ hybridization of oxytocin messenger RNA: macroscopic distribution and quantitation in rat hypothalamic cell groups. Biochem Biophys Res Commun. 1987; 145:10–14. [PubMed: 3593333]

Burbach, JPH., Young, LJ., Russell, JA. Oxytocin: synthesis, secretion, and reproductive functions.. In: Neill, JD., editor. Knobil and Neill's physiology of reproduction. Academic Press; Oxford: 2006.

Caldwell JD, Jirikowski GF, Greer ER, Stumpf WE, Pedersen CA. Ovarian steroids and sexual interaction alter oxytocinergic content and distribution in the basal forebrain. Brain Res. 1988; 446:236–244. [PubMed: 3370488]

Castel M, Morris JF. The neurophysin-containing innervation of the forebrain of the mouse. Neuroscience. 1988; 24:937–966. [PubMed: 3380308]

Christiansen SH. Regulation of the galanin system in the brainstem and hypothalamus by electroconvulsive stimulation in mice. Neuropeptides. 2011; 45:337–341. [PubMed: 21820174]

Ciosek J, Drobnik J. Galanin modulates oxytocin release from rat hypothalamo-neurohypophysial explant in vitro—the role of acute or prolonged osmotic stimulus. Endokrynol Pol. 2013; 64:139–148. [PubMed: 23653277]

Cservenak M, Bodnar I, Usdin TB, Palkovits M, Nagy GM, Dobolyi A. Tuberoinfundibular peptide of 39 residues is activated during lactation and participates in the suckling-induced prolactin release in rat. Endocrinology. 2010; 151:5830–5840. [PubMed: 20861230]

Cservenak M, Szabo ER, Bodnar I, Leko A, Palkovits M, Nagy GM, Usdin TB, Dobolyi A. Thalamic neuropeptide mediating the effects of nursing on lactation and maternal motivation. Psychoneuroendocrinology. 2013; 38:3070–3084. [PubMed: 24094875]

Decavel C, Van den Pol AN. GABA: a dominant neurotransmitter in the hypothalamus. J Comp Neurol. 1990; 302:1019–1037. [PubMed: 2081813]

Decavel C, van den Pol AN. Converging GABA- and glutamate-immunoreactive axons make synaptic contact with identified hypothalamic neurosecretory neurons. J Comp Neurol. 1992; 316:104–116. [PubMed: 1349310]

Diaz-Cabiale Z, Flores-Burgess A, Parrado C, Narvaez M, Millon C, Puigcerver A, Covenas R, Fuxe K, Narvaez JA. Galanin receptor/neuropeptide y receptor interactions in the central nervous system. Curr Protein Pept Sci. 2014; 15:666–672. [PubMed: 25175455]

Didier A, Carleton A, Bjaalie JG, Vincent JD, Ottersen OP, Storm-Mathisen J, Lledo PM. A dendrodendritic reciprocal synapse provides a recurrent excitatory connection in the olfactory bulb. Proc Natl Acad Sci USA. 2001; 98:6441–6446. [PubMed: 11353824]

Dobolyi A. Novel potential regulators of maternal adaptations during lactation: tuberoinfundibular peptide 39 and amylin. J Neuroendocrinol. 2011; 23:1002–1008. [PubMed: 21418340]

Dobolyi A, Ueda H, Uchida H, Palkovits M, Usdin TB. Anatomical and physiological evidence for involvement of tuberoinfundibular peptide of 39 residues in nociception. Proc Natl Acad Sci USA. 2002; 99:1651–1656. [PubMed: 11818570]

Dobolyi A, Palkovits M, Usdin TB. Expression and distribution of tuberoinfundibular peptide of 39 residues in the rat central nervous system. J Comp Neurol. 2003; 455:547–566. [PubMed: 12508326]

Dobolyi A, Irwin S, Wang J, Usdin TB. The distribution and neurochemistry of the parathyroid hormone 2 receptor in the rat hypothalamus. Neurochem Res. 2006a; 31:227–236. [PubMed: 16570212]

Dobolyi A, Wang J, Irwin S, Usdin TB. Postnatal development and gender-dependent expression of TIP39 in the rat brain. J Comp Neurol. 2006b; 498:375–389. [PubMed: 16871538]

Dobolyi A, Palkovits M, Usdin TB. The TIP39-PTH2 receptor system: unique peptidergic cell groups in the brainstem and their interactions with central regulatory mechanisms. Prog Neurobiol. 2010; 90:29–59. [PubMed: 19857544]

Dobolyi A, Grattan DR, Stolzenberg DS. Preoptic inputs and mechanisms that regulate maternal responsiveness. J Neuroendocrinol. 2014; 26:627–640. [PubMed: 25059569]

Dulac C, O'Connell LA, Wu Z. Neural control of maternal and paternal behaviors. Science. 2014; 345:765–770. [PubMed: 25124430]

El-Emam Dief A, Caldwell JD, Jirikowski GF. Colocalization of p450 aromatase and oxytocin immunostaining in the rat hypothalamus. Horm Metab Res. 2013; 45:273–276. [PubMed: 23225240]

Eriksson M, Ceccatelli S, Uvnas-Moberg K, Iadarola M, Hokfelt T. Expression of Fos-related antigens, oxytocin, dynorphin and galanin in the paraventricular and supraoptic nuclei of lactating rats. Neuroendocrinology. 1996; 63:356–367. [PubMed: 8739891]

Fleming AS, Walsh C. Neuropsychology of maternal behavior in the rat: c-fos expression during mother-litter interactions. Psychoneuroendocrinology. 1994; 19:429–443. [PubMed: 7938344]

Freeman ME, Kanyicska B, Lerant A, Nagy G. Prolactin: structure, function, and regulation of secretion. Physiol Rev. 2000; 80:1523–1631. [PubMed: 11015620]

Garcia-Falgueras A, Ligtenberg L, Kruijver FP, Swaab DF. Galanin neurons in the intermediate nucleus (InM) of the human hypothalamus in relation to sex, age, and gender identity. J Comp Neurol. 2011; 519:3061–3084. [PubMed: 21618223]

Gavrilov YV, Ellison BA, Yamamoto M, Reddy H, Haybaeck J, Mignot E, Baumann CR, Scammell TE, Valko PO. Disrupted sleep in narcolepsy: exploring the integrity of galanin neurons in the ventrolateral preoptic Area. Sleep. 2016; 39:1059–1062. [PubMed: 26951397]

Grattan DR, Kokay IC. Prolactin: a pleiotropic neuroendocrine hormone. J Neuroendocrinol. 2008; 20:752–763. [PubMed: 18601698]

Greer ER, Caldwell JD, Johnson MF, Prange AJ Jr, Pedersen CA. Variations in concentration of oxytocin and vasopressin in the paraventricular nucleus of the hypothalamus during the estrous cycle in rats. Life Sci. 1986; 38:2311–2318. [PubMed: 3724360]

Hammouche SB, Bennis M. Galanin immunoreactivity in the brain of the desert lizard Uromastyx acanthinura during activity season. Folia Histochem Cytobiol. 2013; 51:45–54. [PubMed: 23690217]

Hokfelt T, Broberger C, Diez M, Xu ZQ, Shi T, Kopp J, Zhang X, Holmberg K, Landry M, Koistinaho J. Galanin and NPY, two peptides with multiple putative roles in the nervous system. Horm Metab Res. 1999; 31:330–334. [PubMed: 10422730]

Hou-Yu A, Lamme AT, Zimmerman EA, Silverman AJ. Comparative distribution of vasopressin and oxytocin neurons in the rat brain using a double-label procedure. Neuroendocrinology. 1986; 44:235–246. [PubMed: 3540701]

Insel TR, Harbaugh CR. Lesions of the hypothalamic paraventricular nucleus disrupt the initiation of maternal behavior. Physiol Behav. 1989; 45:1033–1041. [PubMed: 2780864]

Jakobowitz, DM., Skofitsch, G. Localization of galanin cell bodies in the brain by immunohistochemistry and in situ hybridization histochemistry.. In: Hökfelt, T.Bartfai, T.Jacobowitz, DM., Ottoson, D., editors. Galanin: a new multifunctional peptide in the neuroendocrine system. Macmillan Press; London: 1991. p. 69-92.

Jenstad M, Quazi AZ, Zilberter M, et al. System A transporter SAT2 mediates replenishment of dendritic glutamate pools controlling retrograde signaling by glutamate. Cereb Cortex. 2009; 19:1092–1106. [PubMed: 18832333]

Knobloch HS, Grinevich V. Evolution of oxytocin pathways in the brain of vertebrates. Front Behav Neurosci. 2014; 8:31. [PubMed: 24592219]

Laflamme N, Nappi RE, Drolet G, Labrie C, Rivest S. Expression and neuropeptidergic characterization of estrogen receptors (ERalpha and ERbeta) throughout the rat brain: anatomical evidence of distinct roles of each subtype. J Neurobiol. 1998; 36:357–378. [PubMed: 9733072]

Landry M, Roche D, Angelova E, Calas A. Expression of galanin in hypothalamic magnocellular neurones of lactating rats: co-existence with vasopressin and oxytocin. J Endocrinol. 1997; 155:467–481. [PubMed: 9487992]

Lang R, Gundlach AL, Kofler B. The galanin peptide family: receptor pharmacology, pleiotropic biological actions, and implications in health and disease. Pharmacol Ther. 2007; 115:177–207. [PubMed: 17604107]

Larsen CM, Grattan DR. Prolactin, neurogenesis, and maternal behaviors. Brain Behav Immun. 2012; 26:201–209. [PubMed: 21820505]

Laurent FM, Hindelang C, Klein MJ, Stoeckel ME, Felix JM. Expression of the oxytocin and vasopressin genes in the rat hypothalamus during development: an in situ hybridization study. Brain Res Dev Brain Res. 1989; 46:145–154. [PubMed: 2706768]

Li C, Chen P, Smith MS. Neural populations in the rat forebrain and brainstem activated by the suckling stimulus as demonstrated by cFos expression. Neuroscience. 1999; 94:117–129. [PubMed: 10613502]

Mann PE, Bridges RS. Prolactin receptor gene expression in the forebrain of pregnant and lactating rats. Brain Res Mol Brain Res. 2002; 105:136–145. [PubMed: 12399116]

Martin-Perez J, Garcia-Martinez JM, Sanchez-Bailon MP, Mayoral-Varo V, Calcabrini A. Role of SRC family kinases in prolactin signaling. Adv Exp Med Biol. 2015; 846:163–188. [PubMed: 25472538]

Mathieson WB, Taylor SW, Marshall M, Neumann PE. Strain and sex differences in the morphology of the medial preoptic nucleus of mice. J Comp Neurol. 2000; 428:254–265. [PubMed: 11064365]

Matsubara A, Laake JH, Davanger S, Usami S, Ottersen OP. Organization of AMPA receptor subunits at a glutamate synapse: a quantitative immunogold analysis of hair cell synapses in the rat organ of Corti. J Neurosci. 1996; 16:4457–4467. [PubMed: 8699256]

Meeker RB, Swanson DJ, Greenwood RS, Hayward JN. Quantitative mapping of glutamate presynaptic terminals in the supraoptic nucleus and surrounding hypothalamus. Brain Res. 1993; 600:112–122. [PubMed: 8093674]

Meister B, Villar MJ, Ceccatelli S, Hokfelt T. Localization of chemical messengers in magnocellular neurons of the hypothalamic supraoptic and paraventricular nuclei: an immunohisto-chemical study using experimental manipulations. Neuroscience. 1990; 37:603–633. [PubMed: 1701038]

Neville, MC. Lactation and Its Hormonal Control.. In: Neill, JD., editor. Physiology of reproduction. Academic Press; Amsterdam: 2006. p. 2993-3054.

Nomura M, Tsutsui M, Shimokawa H, Fujimoto N, Ueta Y, Morishita T, Yanagihara N, Matsumoto T. Effects of nitric oxide synthase isoform deletion on oxytocin and vasopressin messenger RNA in mouse hypothalamus. NeuroReport. 2005; 16:413–417. [PubMed: 15729148]

Numan, M., Insel, TR. The neurobiology of parental behavior. Springer; New York: 2003.

Numan M, Rosenblatt JS, Komisaruk BR. Medial preoptic area and onset of maternal behavior in the rat. J Comp Physiol Psychol. 1977; 91:146–164. [PubMed: 402400]

Nylen A, Skagerberg G, Alm P, Larsson B, Holmqvist B, Andersson KE. Nitric oxide synthase in the hypothalamic paraventricular nucleus of the female rat; organization of spinal projections and coexistence with oxytocin or vasopressin. Brain Res. 2001; 908:10–24. [PubMed: 11457427]

Olazabal DE, Kalinichev M, Morrell JI, Rosenblatt JS. MPOA cytotoxic lesions and maternal behavior in the rat: effects of midpubertal lesions on maternal behavior and the role of ovarian hormones in maturation of MPOA control of maternal behavior. Horm Behav. 2002; 41:126–138. [PubMed: 11855898]

Ottersen OP. Postembedding immunogold labelling of fixed glutamate: an electron microscopic analysis of the relationship between gold particle density and antigen concentration. J Chem Neuroanat. 1989; 2:57–66. [PubMed: 2571347]

Ottersen OP, Storm-Mathisen J, Bramham C, Torp R, Laake J, Gundersen V. A quantitative electron microscopic immunocytochemical study of the distribution and synaptic handling of glutamate in rat hippocampus. Prog Brain Res. 1990; 83:99–114. [PubMed: 1975455]

Paxinos, G., Watson, C. The rat brain in stereotaxic coordinates. Academic Press; Sidney: 1997.

Paxinos, G., Watson, C. The rat brain in stereotaxic coordinates. Academic Press; San Diego: 2007.

Pedersen CA, Caldwell JD, Walker C, Ayers G, Mason GA. Oxytocin activates the postpartum onset of rat maternal behavior in the ventral tegmental and medial preoptic areas. Behav Neurosci. 1994; 108:1163–1171. [PubMed: 7893408]

Pedersen CA, Vadlamudi SV, Boccia ML, Amico JA. Maternal behavior deficits in nulliparous oxytocin knockout mice. Genes Brain Behav. 2006; 5:274–281. [PubMed: 16594980]

Phend KD, Weinberg RJ, Rustioni A. Techniques to optimize post-embedding single and double staining for amino acid neurotransmitters. J Histochem Cytochem. 1992; 40:1011–1020. [PubMed: 1376741]

Porteous R, Petersen SL, Yeo SH, Bhattarai JP, Ciofi P, de Tassigny XD, Colledge WH, Caraty A, Herbison AE. Kisspeptin neurons co-express met-enkephalin and galanin in the rostral periventricular region of the female mouse hypothalamus. J Comp Neurol. 2011; 519:3456–3469. [PubMed: 21800299]

Powers-Martin K, Phillips JK, Biancardi VC, Stern JE. Heterogeneous distribution of basal cyclic guanosine monophosphate within distinct neuronal populations in the hypothalamic paraventricular nucleus. Am J Physiol Regul Integr Comp Physiol. 2008; 295:R1341–R1350. [PubMed: 18703416]

Rhodes CH, Morrell JI, Pfaff DW. Immunohistochemical analysis of magnocellular elements in rat hypothalamus: distribution and numbers of cells containing neurophysin, oxytocin, and vasopressin. J Comp Neurol. 1981; 198:45–64. [PubMed: 7014660]

Rossmanith WG, Clifton DK, Steiner RA. Galanin gene expression in hypothalamic GnRH-containing neurons of the rat: a model for autocrine regulation. Horm Metab Res. 1996; 28:257–266. [PubMed: 8811325]

Sapsford TJ, Kokay IC, Ostberg L, Bridges RS, Grattan DR. Differential sensitivity of specific neuronal populations of the rat hypothalamus to prolactin action. J Comp Neurol. 2012; 520:1062–1077. [PubMed: 21953590]

Simerly RB, Swanson LW. The organization of neural inputs to the medial preoptic nucleus of the rat. J Comp Neurol. 1986; 246:312–342. [PubMed: 3517086]

Simerly RB, Swanson LW. Projections of the medial preoptic nucleus: a Phaseolus vulgaris leucoagglutinin anterograde tract-tracing study in the rat. J Comp Neurol. 1988; 270:209–242. [PubMed: 3259955]

Simmons DM, Swanson LW. High-resolution paraventricular nucleus serial section model constructed within a traditional rat brain atlas. Neurosci Lett. 2008; 438:85–89. [PubMed: 18479821]

Sjoeholm A, Bridges RS, Grattan DR, Anderson GM. Region-, neuron-, and signaling pathway-specific increases in prolactin responsiveness in reproductively experienced female rats. Endocrinology. 2011; 152:1979–1988. [PubMed: 21363933]

Somogyi P, Halasy K, Somogyi J, Storm-Mathisen J, Ottersen OP. Quantification of immunogold labelling reveals enrichment of glutamate in mossy and parallel fibre terminals in cat cerebellum. Neuroscience. 1986; 19:1045–1050. [PubMed: 2881226]

Stack EC, Numan M. The temporal course of expression of c-Fos and Fos B within the medial preoptic area and other brain regions of postpartum female rats during prolonged mother–young interactions. Behav Neurosci. 2000; 114:609–622. [PubMed: 10883811]

Stern JM, Lonstein JS. Neural mediation of nursing and related maternal behaviors. Prog Brain Res. 2001; 133:263–278. [PubMed: 11589136]

Storm-Mathisen J, Leknes AK, Bore AT, Vaaland JL, Edminson P, Haug FM, Ottersen OP. First visualization of glutamate and GABA in neurones by immunocytochemistry. Nature. 1983; 301:517–520. [PubMed: 6130475]

Strathearn L, Fonagy P, Amico J, Montague PR. Adult attachment predicts maternal brain and oxytocin response to infant cues. Neuropsychopharmacology. 2009; 34:2655–2666. [PubMed: 19710635]

Szabo FK, Snyder N, Usdin TB, Hoffman GE. A direct neuronal connection between the subparafascicular and ventrolateral arcuate nuclei in non-lactating female rats. Could this pathway play a role in the suckling-induced prolactin release? Endocrine. 2010; 37:62–70. [PubMed: 20963557]

Tillet Y, Tourlet S, Picard S, Sizaret PY, Caraty A. Morphofunctional interactions between galanin and GnRH-containing neurones in the diencephalon of the ewe. The effect of oestradiol. J Chem Neuroanat. 2012; 43:14–19. [PubMed: 21983419]

Torner L, Toschi N, Nava G, Clapp C, Neumann ID. Increased hypothalamic expression of prolactin in lactation: involvement in behavioural and neuroendocrine stress responses. Eur J Neurosci. 2002; 15:1381–1389. [PubMed: 11994132]

Usdin TB, Hoare SR, Wang T, Mezey E, Kowalak JA. TIP39: a new neuropeptide and PTH2-receptor agonist from hypothalamus. Nat Neurosci. 1999; 2:941–943. [PubMed: 10526330]

Wang BL, Larsson LI. Simultaneous demonstration of multiple antigens by indirect immunofluorescence or immunogold staining. Novel light and electron microscopical double and triple staining method employing primary antibodies from the same species. Histochemistry. 1985; 83:47–56. [PubMed: 2412988]

Whitelaw CM, Robinson JE, Hastie PM, Padmanabhan V, Evans NP. Effects of cycle stage on regionalised galanin, galanin receptors 1–3, GNRH and GNRH receptor mRNA expression in the ovine hypothalamus. J Endocrinol. 2012; 212:353–361. [PubMed: 22159505]

Wu Z, Autry AE, Bergan JF, Watabe-Uchida M, Dulac CG. Galanin neurons in the medial preoptic area govern parental behaviour. Nature. 2014; 509:325–330. [PubMed: 24828191]

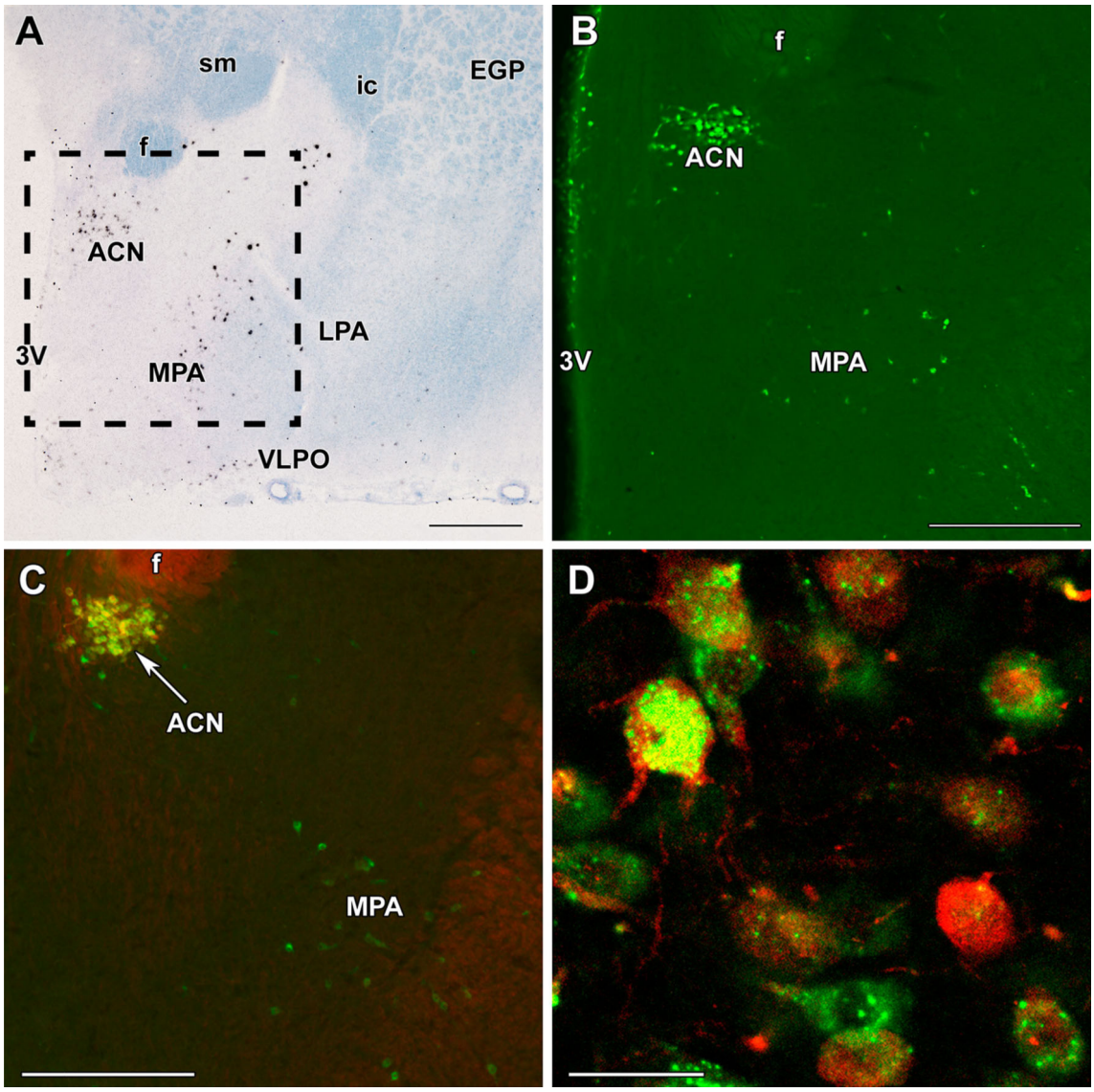

Fig. 1.

Galanin neurons in the preoptic area and their oxytocin content. **a** A bright-field in situ hybridization histochemistry image at bregma level −0.9 mm demonstrates the presence and distribution of galanin mRNA-expressing cells (*black* signal) in the preoptic area of a mother rat. **b** A picture of a galanin-immunolabeled section corresponding to the framed area in **a** is shown. **c** Oxytocin immunoreactivity (*red*) is present in galanin neurons (*green*) of the anterior commissural nucleus (*ACN*), but not in the medial preoptic area (MPA). **d** A high-magnification confocal image demonstrates the double labeling of neurons in the ACN. Note the different distributions of galanin and oxytocin immunoreactivity in the cell bodies and the oxytocin labeling of proximal dendrites. *f* fornix, *ic* internal capsule, *EGP* external globus pallidus, *LPA* lateral preoptic area, *sm* stria medullaris, *VLPO* ventrolateral preoptic nucleus, *3V* third ventricle. *Scale bars* 500 μm for **a**, 400 μm for **b** and **c**, and 40 μm for **d**

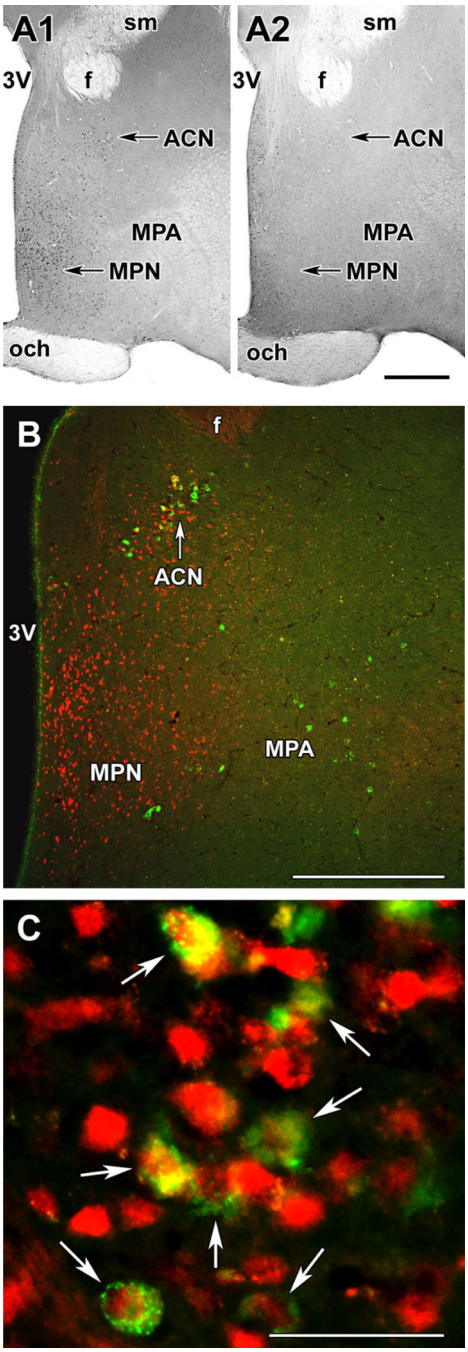

Fig. 2.

Presence of pSTAT5 in preoptic galanin neurons. **a** pSTAT5 immunoreactivity in the preoptic area. **a1** pSTAT5-positive cells in mother rat 2 h after the start of suckling. **a2** pSTAT5 immunoreactivity in mother rats deprived of their pups for 24 h. pSTAT5-ir neurons are abundant in the medial preoptic nucleus (*MPN*) and the area dorsal to it, including the anterior commissural nucleus (*ACN*). In contrast, only a few pSTAT5-ir neurons are present in the medial preoptic area (*MPA*) lateral to the MPN. **b** Galanin-ir neurons (*green*) are present in the ACN and in the MPA, where pSTAT5-ir (*red*) neurons are also present 2 h

after the start of suckling. **c** A high-magnification confocal image demonstrates that in the ACN, the majority of galanin-ir neurons contain pSTAT5 immunoreactivity (white arrows). *f* fornix, *och* optic chiasm, *sm* stria medullaris, *3V* third ventricle. *Scale bars* 500 μm for **a** and **b**, and 50 μm for **c**

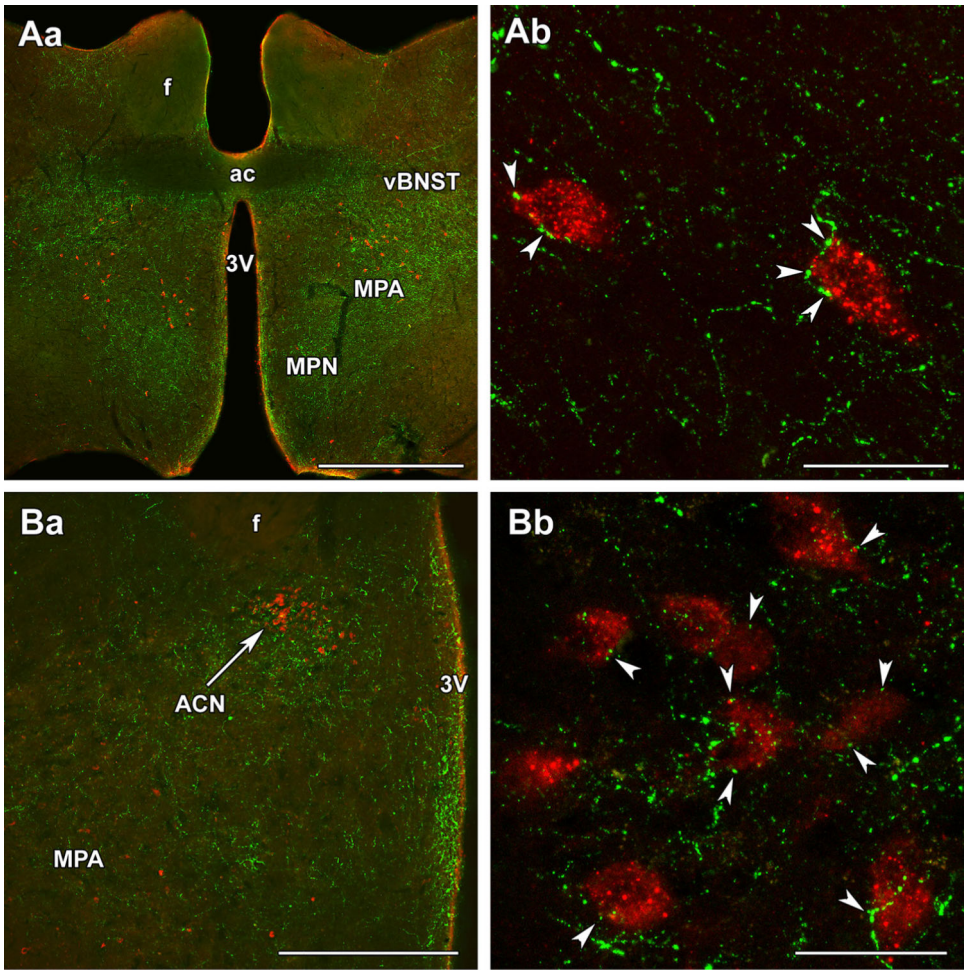

Fig. 3.

Topographical relationship between TIP39 fibers and galanin neurons in the preoptic area of mother rats. **Aa** TIP39 fibers (*green*) are located in the medial preoptic nucleus (*MPN*), medial preoptic area (*MPA*), and the ventral subdivision of the bed nucleus of the stria terminalis (*vBNST*) at the caudal level of the anterior commissure (*ac*). In the MPA, TIP39 fibers are located around galanin neurons (*red*). **Ab** A high-magnification confocal image demonstrates that galanin-ir neurons are closely apposed by TIP39 varicosities in the MPA. **Ba** The anterior commissural nucleus (*ACN*) is visible in the dorsal part of a more caudal level of the preoptic area. **Bb** Galanin neurons in the ACN are also closely apposed by TIP39 varicosities (*white arrowheads*). *f* fornix, *3V* third ventricle. *Scale bars* 1 mm for **Aa**, 50 μm for **Ab**, 500 μm for **Ba**, and 50 μm for **Bb**

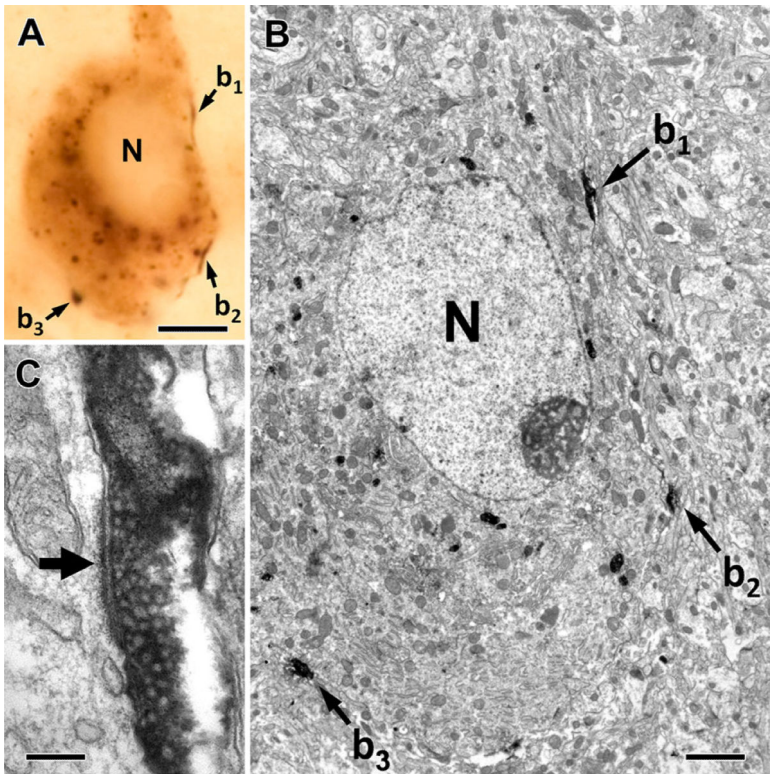

Fig. 4.

TIP39-positive thalamic axons innervate galanin neurons in the MPA. Correlated light and electron micrographs of a galaninimmunoreactive cell that receives three contacts from TIP39-positive thalamic boutons (*b1–b3*) in the plane of the section. The low-power (**a**) and high-power micrographs (**b, c**) verify that the conventional asymmetrical synapses are established on the soma of the galaninimmunoreactive cell as demonstrated by the long post-synaptic specialization (*filled arrow*) of the synapse formed by a TIP39-positive terminal (*b1*) in **c**. *N* nucleus. *Scale bars* 5 μm for **a**, 2 μm for **b**, and 200 nm for **c**

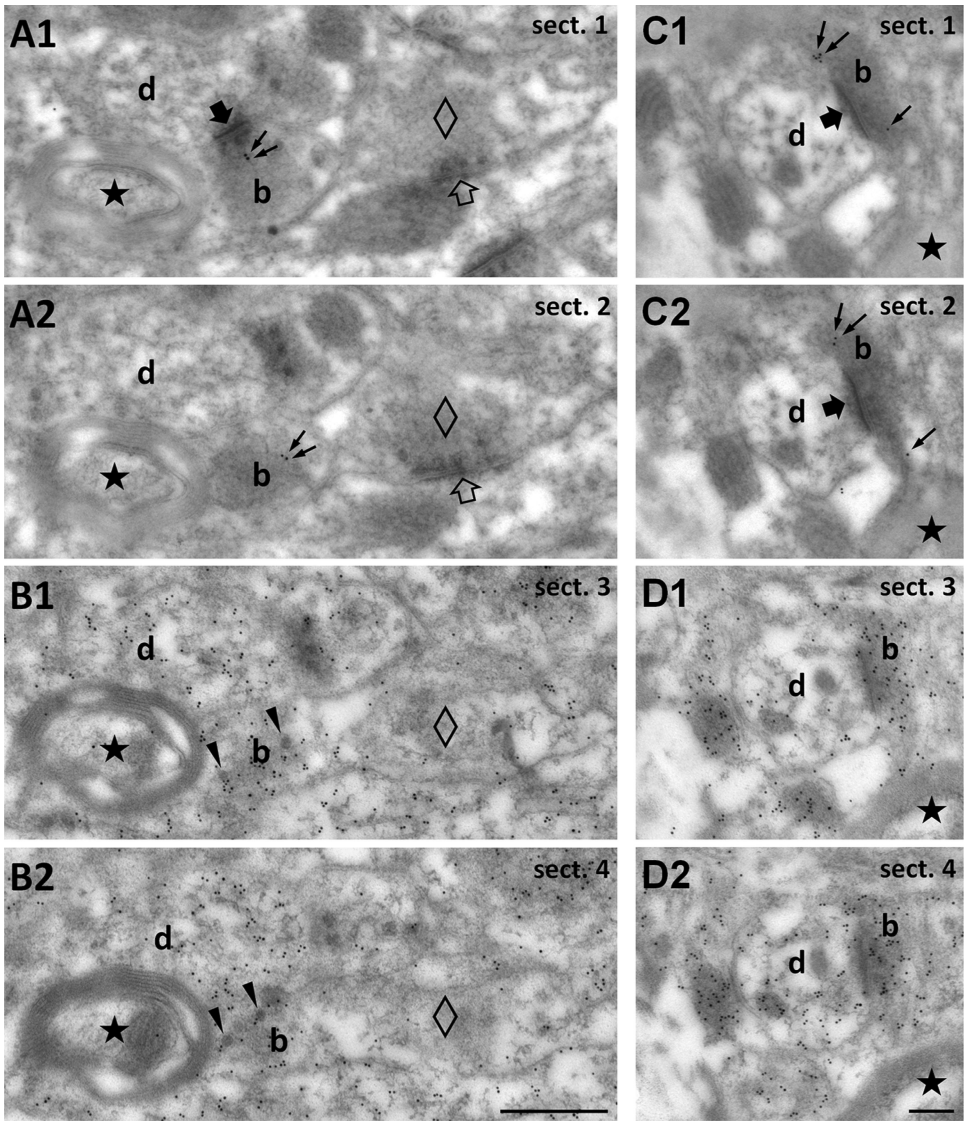

Fig. 5.

Demonstration of the glutamate content of TIP39 terminals in the MPA using consecutive serial electron micrographs sections. **a1, a2** Consecutive sections (sect. 1–4) labeled for TIP39 to demonstrate TIP39 immunoreactivity (10 nm gold particles, *small black arrows*) in a bouton (*b*) establishing asymmetric synapse (*large filled arrow* visible only in **a1**) with a thin, unlabeled dendrite (*d*). Note that TIP39 immunoreactivity is absent from putative inhibitory terminals (*empty diamond*) establishing a symmetric synapse (*empty arrow*) on a dendrite. **b** Immunogold labeling for glutamate (10 nm gold particles) demonstrates that glutamate is enriched in the TIP39-immunopositive terminal seen in **a**. The *black star* shows a myelinated axon as one of the markers that demonstrate that sections in **b** are consecutive to those in **a**. In addition, note the presence of dense core vesicles (*black arrowheads*) implying neuropeptide content in the TIP39-positive terminal. The bouton that establishes symmetric (putative inhibitory) synapse seen in **a** (*empty diamond* in all *panels*) and the myelinated axon (*black star*) do not accumulate glutamate. **c, d** Another example of a

glutamatergic TIP39 terminal shown in consecutive serial sections. **c1** and **c2** are immunolabeled for TIP39, while **d1** and **d2** are labeled for glutamate. *Scale bar* 500 nm for **a** and **b,** and 200 nm for **c** and **d**

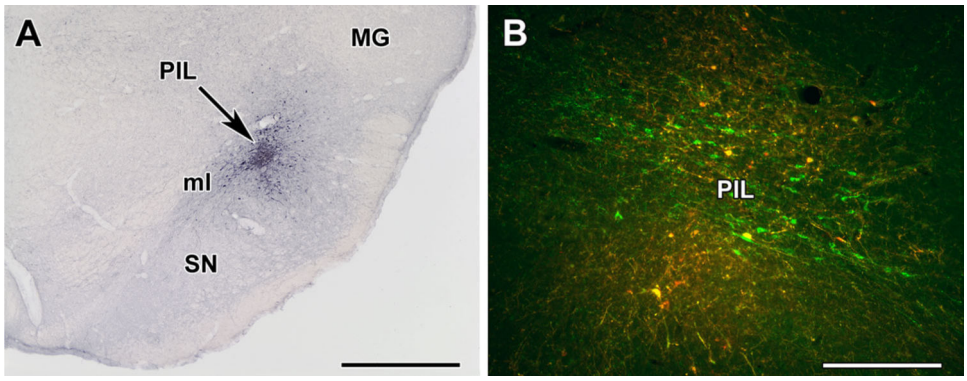

Fig. 6.

Injection of the anterograde tracer biotinylated dextran amine (*BDA*) into the posterior intralaminar complex of the thalamus (*PIL*). **a** Injection site (*black arrow*) is shown in the PIL. **b** Some TIP39 neurons (*green*) take up the BDA (*red*) in and around the injection site (double-labeled *yellow* cells). *MG* medial geniculate body, *ml* medial lemniscus, *SN* substantia nigra. *Scale bars* 1 mm for **a,** and 400 lm for **b**

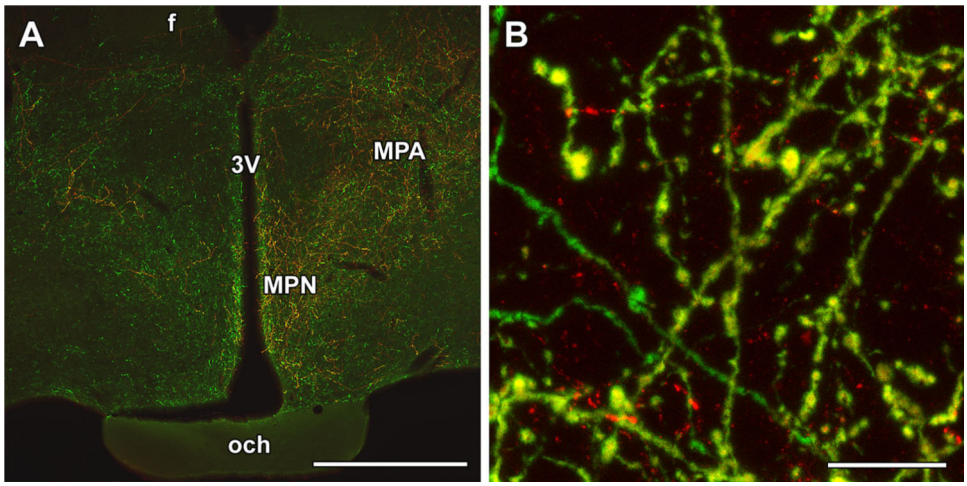

Fig. 7.

Anterogradely labeled fibers in the preoptic area following injection of biotinylated dextran amine (BDA) into the posterior intralaminar complex of the thalamus (PIL). **a** A high density of BDA-labeled (*red*) fibers appear in the preoptic area ipsilateral to the injection site, while a few BDA fibers are also present in the contralateral side. The distribution of the anterogradely labeled neuronal fibers is similar to that of TIP39-ir (*green*) fibers in the preoptic area. **b** A high-magnification confocal image demonstrates that double-labeled fibers (*yellow*) are intermixed with the single-labeled ones. *f* fornix, *MPA* medial preoptic area, *MPN* medial preoptic nucleus, *och* optic chiasm, *3V* third ventricle. *Scale bars* 1 mm for **a,** and 30 μm for **b**